NorCal Open Access Publications
Journal of Environmental Science and Allied Research
Volume 1; Issue 1
Lein JK and Hong X

Research Article

Fingerprinting Anthropogenic "Waste" Heat Across an Urban Landscape Using Earth Observational Satellite Data

James K Lein[1*] and Xin Hong[2]

[1]Department of Geography, Ohio University, Athens, Ohio, USA
[2]Department of Geography, Kent State University, Kent, Ohio, USA

[*]**Corresponding author:** James K Lein, Department of Geography, Ohio University, Athens, OH 45701, USA, Tel: +1 7405931147; E-mail: lein@ohio.edu

Received Date: 21 June, 2017; **Accepted Date:** 30 July, 2017; **Published Date:** 17 August, 2017

Abstract

The impact of urbanized areas on local climate is a well-documented phenomenon. Through the application of remote sensing technologies, the impact of the city landscape can be observed over a larger spatial extent. As interest in promoting environmental sustainability continues to grow, there is a desire to identify methods to reduce the adverse consequences of urbanization. In this study the problem of urban thermal pollution was examined. Focusing on the measurement and mapping of anthropogenic waste heat, this study employed a "snap-shot" analysis at regional scale of the waste heat/land cover associations using data acquired from the Landsat 8 Operational Land Imager (OLI) and Thermal Infrared Sensor (TIRS) earth observational satellite. The "snap-shot" method documented zones in the region of extreme patterns of waste heat and facilitated the "fingerprinting" of waste heat patterns to specific categories of land cover using GIS. The resulting fingerprints delineated areas in the study area where land cover configurations produced excesses of waste heat and served to identify potential targets for waste heat mitigation activities.

Keywords

Pollution Fingerprinting; Thermal Remote Sensing; Urban Land Cover Analysis; Waste Heat

Introduction

The relationship between urban land cover and elevated surface temperatures has been documented in the literature for well over forty years [1,2]. With the advent of satellite-based thermal sensors new techniques have been introduced to capture the heating effects related to the surface radiative and thermodynamic properties of the urban surface. These studies have contributed to a deeper understanding of the role urban land transformations play with respect to unique attributes such as energy consumption, ecosystem function, human health and components that define local micro-climates [3]. More recently, interest has focused on the question of urban thermal pollution and the application of remotely sensed data as an assessment tool [4]. Urban thermal pollution is known to be strongly associated with increases in ambient temperatures at both local and regional scales [5]. The intensification of urban land cover and its spread exacerbates thermal pollution, which is closely related to the urban heat island effect. Anthropogenic heat, produced by the material fabric of the urban surface and the pace and form of human activities common to this landscape has become an important focal point in the drive to improve the environmental sustainability of the city [6].

One approach to address the adverse impacts of urban thermal pollution and enhance urban sustainability concentrates effort on the extent and distribution of green space as a mitigating agent [7]. The composition and configuration of the urban surface creates a complex spatial pattern with contrasting densities, building heights, materials and uses together with a variable mix of vegetative and non-vegetative areas whose configuration and densities also show substantial spatial variation. Surface complexity frustrates planning efforts aim at mitigating urban heat island effects and target areas where the generation of urban waste heat can be reduced [8,9]. A tractable methodology is required to support planning efforts to address urban thermal pollution, guide mitigation and combat waste-heat generation.

Objectives

The purpose of this paper is to demonstrate an approach to "finger print" sources of urban "waste heat" through the application of moderate resolution remotely sensed data. Applying thermal remote sensing in scientific investigations of the urban heat island effect can be involved and expensive undertakings [10]. Cost and complexity issues frustrate wide-spread application of this technology. Limitations stems largely from data collection issues related to the orbital

parameters that define how earth observational satellites function, earth observational systems explain a re-visit period that do not permit the collection of a steady stream of imagery over the urban surface. Furthermore, clouds and atmospheric interactions together with short dwell times over a target conspire to reduce image fidelity. However, the main technical concern with satellite-based observations is that the surface temperatures acquired by a sensor only describe the spatial pattern of upward thermal radiance as received by the satellite platform [10,11]. Given this imperfect setting, the challenge is to exploit the capabilities of satellite systems and develop useful approaches that deliver actionable information to decision makers. The methodology demonstrated in this paper begins these processes by first relaxing the requirements typical of a scientific study of the urban heating effect. Rather, research presented in this paper centers on mapping thermal waste heat pollution by adopting a "snap-shot" perspective that detects and quantifies areas where thermal patterns identify conditions that exceed ambient temperature characteristics. By delineating zones in the urban surface that identify sources of waste heat, the pattern of excess heating can be related back to specific land covers and candidate locations can be targeted mitigation. The product of this methodology, facilitates the synoptic-scale comparison of waste heat patterns with urban land cover that can be linked to more specific land use and ownership data to guide planning efforts in a GIS environment.

The Mechanics of Urban Heating and Mitigation

When compared to natural landscape, the artificial features and arrangements of the built environment establish unique surface energy flows [12-14]. The behavior of net radiation when encountering the texture and material composition of urban land modifies the absorption of short-wave and long-wave radiation, transpiration and evaporation rates, surface energy storage and the flux of latent and sensible heat transfer. Add to these conditions the contribution of anthropogenic heat, and the blocking and shielding effects of urban terrain, and a pattern of local climate is produced that is substantially different from less urbanized surfaces. This condition has been modeled as the urban energy budget and expressed symbolically according to the relationship:

$$Q^* + Qf = Qh + Qe + \Delta Qs + \Delta Qa \quad (1)$$

Where Q* defines net radiation, Qh and Qe explain the fluxes of sensible and latent heat respectively, Qf represents anthropogenic energy releases and ΔQa describes net advection across the surface and ΔQs represents energy storage. Each term identified in (Equation 1) are functions of the spatial arrangement, density, geographic location and the built characteristics of urban form. Those dependencies suggest that the energy balance and micro-climate will exhibit variability from city to city as these parameters respond to local conditional influences. Therefore while urban surface display a micro-climate different from its surroundings, the intensity of that contrast will reveal measurable spatial and temporal differences [3].

Under ideal conditions the urban heating effect can produce thermal patterns between 10 - 15 oC above those of surrounding land areas, increasing energy demand for cooling and degrading human comfort during summer seasons while reversing these characteristics for winter months [11]. The range of temperature increase and its spatio-temporal variation depends largely on a set of casual factors descriptive of an urbanized landscape [8]:

- Reduced vegetative surface that retards evapotranspiration
- Low albedo materials that enhance the absorption of solar radiation
- Increased surface roughness that modifies air flow, and
- Increased anthropogenic heat releases

Each of these actors explain conditions common to the transformation of a "natural" surface as a region undergoes urbanization. As the pace of urbanization continues a wider range of casual conditions adds additional influence to the urban heating pattern (Table 1).

Low albedo materials
Population concentrations
Destruction of vegetation
Urban canopy effects
Wind blocking
Air pollutants
Energy consumption

Table 1: Conditions that influence urban heating.

Placing these actors into a process oriented design of cause and effect suggests pathways for mitigation (Figure1).

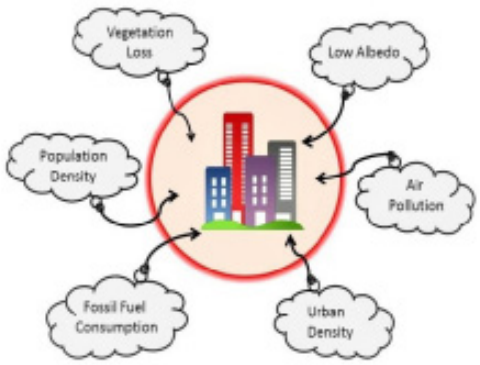

Figure 1: Factors contributing to the urban heating process.

Mitigation strategies

As urban sustainability programs gain traction, there is renewed interest in addressing the problem of urban thermal pollution [15]. Mitigation efforts tend to follow one of four primary pathways: 1) increasing the albedo (reflectivity) of urban surface, 2) increasing

evapotranspiration through urban 'greening', 3) modifying the morphology of the urban surface through urban design, or 4) improving urban energy efficiencies [16,17]. Since buildings and other engineered structure that comprise the urban landscape are the principal targets of mitigation, the spatial configuration and material composition of the built environment plays an integral role in improving urban environmental quality [17]. As noted by Santamouris et al., increased urban temperatures exacerbate the consumption of energy for cooling purposes, increase peak energy demand, intensify ground level pollution and contribute to human discomfort [18]. Materials used in the building envelop and the configuration of urban structures work in concert to absorb solar and infrared radiation and dissipate part of the accumulated heat through convective and radiative processes. The net result is an increase in surrounding ambient temperature. Combating systematic ambient temperature differences across the urban surface requires the adoption of sustainable design and land development innovations [19-21]. In the majority of instances, mitigation measures rely on off-setting the urban-induced modifications of the surface energy balance. Common strategies include:

- Modifying urban morphology and form by reducing building densities and heights, and orienting structures to redirect and improve airflow [17].
- Expand urban green-scape through the elimination of impervious surfaces and by incorporating greenspace and vegetated areas with the built environment [22,23].
- Adopting highly reflective (cool materials) in construction. Cool materials, particularly those employed in roofing or road surfacing, define high solar reflectance characteristics and/or high infrared emittance offering a high surface cooling potential during summer periods [19].
- Implementing green roof programs based on the recognition that a substantial fraction (20-25%) of the exposed urban surface is composed on roof tops [24]. A green or living roof, explains a surface that is partially or completely covered in vegetation. Numerous cities have explored opportunities to encourage retro-fitting exiting rooftops with green roof systems and a means to reduce heating and increase evaporative cooling [23,25].

Mitigating the extremes of urban heating and adopting effective implementation programs remains a challenge. While research on the topic of urban heating provides clear evidence of the problem and offers guidance toward feasible solutions, address the more pragmatic needs of local government decision makers remains elusive. Integrating research findings with urban design and other planning strategies depends on developing programs that can identify and prioritize, on a cost-effective basis, where, in the urban pattern, should mitigation focus. Areas within the urban system that describe extremes of waste heat are not evenly distributed spatially. Therefore, "hot spots" or concentrations of excess heat can be observed primarily where built form densities are high and vegetative surface is minimal or absent. The identification of waste heat hot spots, however, is methodologically involved particularly. Through the application of satellite remote sensing, a thermal characterization of the urban landscape can be acquired that offers a useful "snap-shot" in time of land surface temperatures over a comparative large geographic area. Using that satellite-derived land surface temperature "snap-shot" as a surrogate for ambient air temperature it becomes possible to "fingerprint" regions of thermal excess and establish mitigation priorities around those targeted areas.

Thermal fingerprinting

The "fingerprinting" concept has been adapted to the science of remote sensing from the field of environmental forensics [26]. Fingerprinting is a general term that includes techniques developed to identify specific associations between patterns of a material sample and sources of pollutants within a given environmental setting that may be responsible for the observed contamination. Fingerprinting is an integral activity of environmental forensics; a field that seeks to: 1) systematically examine environmental data to ascertain the source of contaminant release, 2) identify the timing of pollutant releases, 3) define the concentration of contamination and 4) determine the entities responsible for the observed pollution. Adapting these activities to the question of thermal excess or urban waste heat pollution introduces an important spatial component to the fingerprinting concept that can addressed using remote sensing methods.

Utilizing remotely sensed data in a fingerprinting application documents the geographic locations of observed anomalies. While this approach is somewhat of a departure from traditional remote sensing studies where land cover classification takes priority, fingerprinting capitalizes on the generation of information to investigate a specific event or condition and place it in its spatial context. In the example of waste heat pollution, analysis centers on two questions; 1) where are the thermal patterns in excess of ambient conditions, and 2) what land surface characteristics are producing those patterns? With this information, the broad spatial pattern is documented and mitigation priorities can be established.

Methodology

To demonstrate waste heat fingerprinting over an expansive urban surface, a Landsat 8 Operational Land Imager (OLI) and Thermal Infrared Sensor (TIRS) images were acquired for September 14, 2015 for a region in northeast Ohio (path 19, row 31). The Landsat 8 scene was subset and clipped to conform to the administrative boundary of Cuyahoga County Ohio which served as the study area for this analysis (Figure 2). The study region represents a densely populated urban setting with a wide mix of land uses and cover types that provide contrasting surface arrangements to evaluate. The September date selected for this study was the optimal cloud free image that was temporally closest to dates in late August that typically define the region's period of maximum heating. The maximum daily temperature for the study area was taken from the National Center for Environmental Information archive for Cleveland Hopkins International Airport and Cleveland Burke Lakefront Airport. Temperature values for these two recording stations were averaged and assumed constant over the study area. With a thermal profile established, remote sensing analysis could be undertaken.

Figure 2: Study area location and regional setting.

The Landsat 8 TIRS sensor has two thermal infrared channels (Band 10 and Band 11 respectively). For the purposes of this study Landsat 8 thermal infrared Band 10 was chosen to provide estimates of land surface temperature. The process involved in transforming the digital values of brightness in the band 10 image to land surface temperature. Image analysis was conducted using ENVI 5.1 and can be summarized according to a sequence of steps as illustrated in (Figure 3).

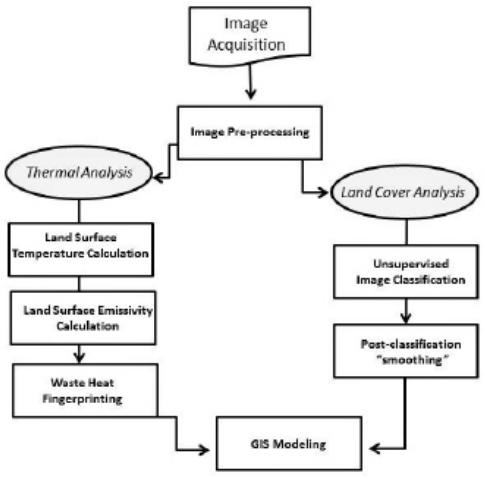

Figure 3: Thermal fingerprinting analysis workflow.

Image pre-processing

Pre-processing prepared the raw satellite image for analysis. Three operations were performed: 1) radiometric calibration, 2) geometric rectification and 3) atmospheric correction. Radiometric calibration involved converting the raw digital numbers of the Landsat 8 scene to at-satellite radiance values. The at-satellite radiance is computed using the calibration values for gain and offset read from the image metadata file. Those equations are provided in (Table 2).

$$L(\lambda) = gain * Qdn + bias$$

$$Gain = \frac{((Lmax(\lambda)-Lmin(\lambda)))}{(Qmax-Qmin)}$$

where $L_{(\lambda)}$ is the spectral radiance of the thermal band detected by the sensor in watts/(meter squared ster*μm); Q_{max} is the maximum quantized calibrated DN with Q_{max} =255; Q_{dn} is the DN value of the grey level of the image; $L_{max(\lambda)}$ and $L_{min(\lambda)}$ are the maximum and minimum received spectral radiance values which are Q_{dn} =0 and Q_{max} =255, respectively. $L_{max(\lambda)}$ and $L_{min(\lambda)}$ values can be found in the Landsat header file.

Table 2: Landsat 8 gain and offset calculation.

Atmospheric correction was accomplished using the histogram minimum method. This technique assumes that the atmosphere is uniform across the scene. Therefore, a dark object (such as a shadow) should have a digital value of zero on the image. If the observed value appears substantially larger than zero, the difference in considered a function of atmospheric scattering. That difference is then subtracted from all pixel values in the image. Geometric rectification involved two operations: 1) registering the image to a geographic grid and 2) performing an image subset to clip the study area from the main scene using a vector file outlining the administrative boundary of the study area.

Calculating estimates of land surface temperature

With the image transformed to units of radiance, surface temperature estimation followed the procedure outlined by Avdan and Jovanovska, and Weng et al., [27,28]. Converting radiance to temperature first required calculating at-sensor temperature (brightness temperature, BT) according to the formula:

$$BT = \frac{K_2}{Ln(K_1/L_\lambda+1)} - 273.15 \quad (2)$$

where K_1 and K_2 are pre-launch calibration values and L is the spectral radiance of the thermal band.

Next, calculating land surface emissivity by obtaining the Normalized Difference Vegetation Index (NDVI) for the surface based on the relation [29]

$$NDVI_{Landsat\ 8} = (Band\ 5 - Band\ 4) / (Band\ 5 + Band\ 4) \quad (3)$$

Then approximating the Proportion of vegetation (Pv) for each pixel in the scene based on:

$$P_v = \left[\frac{NDVI - NDVI_{min}}{NDVI_{max} - NDVI_{min}}\right]^2 \quad (4)$$

With these values an emissivity surface (ε) could be determined using the equation:

$$\varepsilon = \varepsilon_{v\lambda} Pv + \varepsilon_{s\lambda}(1-Pv) + C\lambda \quad (5)$$

Finally, with these parameters in place, Land Surface Temperature (LST) in degrees celsius was determined by:

$$LST = BT/[1+\lambda*(BT/p)*\ln(\varepsilon)] \quad (6)$$

where λ is set to 10.895, ε is the value of emissivity, p is set to 14380 and BT is the estimated value of brightness temperature.

Land cover assessment

To support the task of connecting specific thermal fingerprints with specific land cover arrangements, an unsupervised image classification was performed. For this study, unsupervised classification employed the method of K-means clustering to group pixel brightness values into homogeneous natural (numerical) groupings [26]. Landsat 8 bands 2, 3 and 5 were used for this purpose with an initial cluster seed set to fifteen. These based defined the most optimal combinations based on histogram analysis. These initial clusters were then merged and reclassified manually into seven land cover categories. An accuracy assessment of the land cover surface was undertaken using validation samples acquired from NAPP imagery for a portion of the study area. The results of the validation test are given in (Table 3).

	Observed Class								
Predicted Class	**Industrial and Commercial Complexes**	**Residential**	**Road**	**Forest Land**	**Water**	**Grass/ Agricultural Land**	**Bare Soil**	**No. of classified pixels**	**User's Accuracy**
Industrial and Commercial Complexes	40	0	0	0	0	0	0	40	100%
Residential	0	40	0	0	0	0	0	40	100%
Road	1	0	39	0	0	0	0	40	97.50%
Forest Land	0	0	0	39	0	1	0	40	97.50%
Water	10	0	0	0	30	0	0	40	75%
Grass / Agricultural Land	0	0	0	0	0	40	0	40	100%
Bare Soil	12	0	3	1	0	0	24	40	60%
No. of ground truth pixels	63	40	42	40	30	41	24	280	
Producer's accuracy	63.50%	100%	92.90%	97.50%	100%	97.60%	100%		
Overall Accuracy	90%								
Kappa	88%								

Table 3: Land Cover Accuracy Assessment Land cover accuracies were considered sufficient to facilitate reasonable assessment of waste heat relation to land cover type and patterns of human activity.

Results

The concept of waste heat was suggested by Hey et al., [30]. The underlying premise supporting the formation of waste heat is based on the assumption that given a remotely sensed temperature surface, the value of each pixel in the scene explains an estimate of kinetic temperature radiating skyward. Any pixel in the image with a thermal condition above the nominal ambient air temperature recorded at the approximate time of satellite overpass explains waste or excess heat. Using recorded ambient air temperature over a study site, waste heat can be expressed as:

Waste Heat = Pixel Temperature - Ambient Air Temperature (7)

According to this relationship, waste heat represents heated air that is modifying its surroundings, contributing to warmer conditions that may influence energy demand, human comfort and related conditions indicative of the urban impact of micro-climate. Waste heat values that deviate from ambient conditions, therefore identify opportunities for mitigation. Employing the synoptic-scale vantage-point of an earth observational sensor, a pattern of waste heat can be calculated and examined over a comparative large urban area.

The satellite-derived distribution of Land Surface Temperature (LST) for the Cuyahoga County study area is given in figure 4b with its accompanying land cover surface presented in figure 4a. Land surface temperature radiates outward in a near concentric pattern from the core of urban built form focused on the city of Cleveland. The pattern moderates outward from the urban core with ribbons of cooler temperatures that correspond with riparian corridors and tree covered areas. Variations in the density and form of the built environment are evidences by temperature

patterns that range between 20 to 23°C. The 2015 land cover surface when viewed in combination with LST reveals islands of heating that characterize areas of increased urban densities around sub-urban core parcels, industrial and commercial complexes and following the linear pattern of elevated temperature along major transportation arteries.

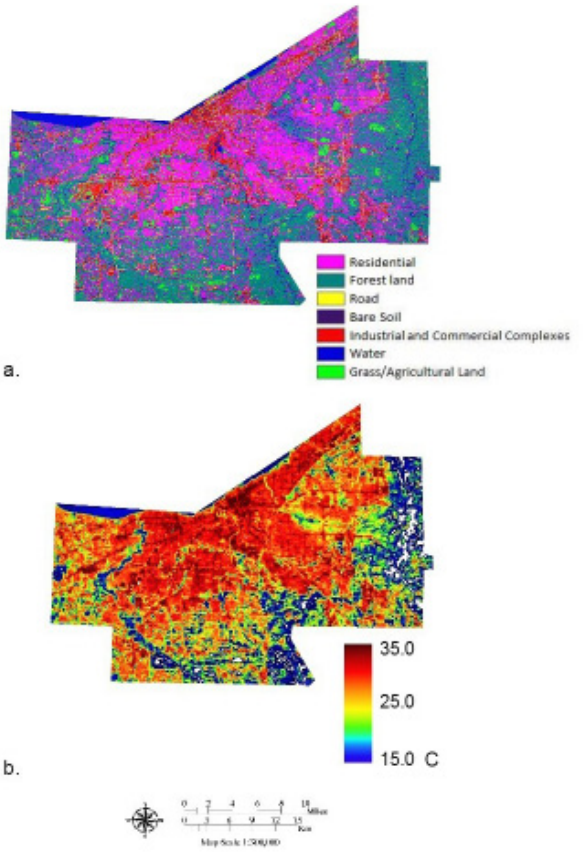

Figure 4: Spatial distribution of a) land cover and b) land surface temperature.

Ambient air temperature for the study area for the September 14, 2015 date at the approximate time of satellite overpass was 23.5°C. Applying this value in the estimating waste heat equation (equation 7) produced a waste heat or excess heating pattern shown in figure 5. Waste heat values ranged from -5°C below ambient air temperature to maximum values from 7 to as high as 20°C for the September 14th date. Excess heat peaks over densely built-up and impervious surface and declines over vegetated areas.

Fingerprinting the sources of waste heat peaks in relation to land cover was accomplished by first breaking the larger Cuyahoga study area into a smaller analytic window displaying land cover and waste heat (Figures 6 and 7). This was done primarily to facilitate visualization of the pattern. Using this window, the waste heat and land cover layers were passed to GIS for analysis. Two basic GIS operations were performed using the Idrisi TerrSet geographic analysis system. First, the analytic window for waste heat was reclassified into four waste heat categories (Table 4). The intervals selected suggest surfaces that trend upward from areas below ambient temperatures, increasing one standard deviation to zones 10 to 20°C above ambient air temperature.

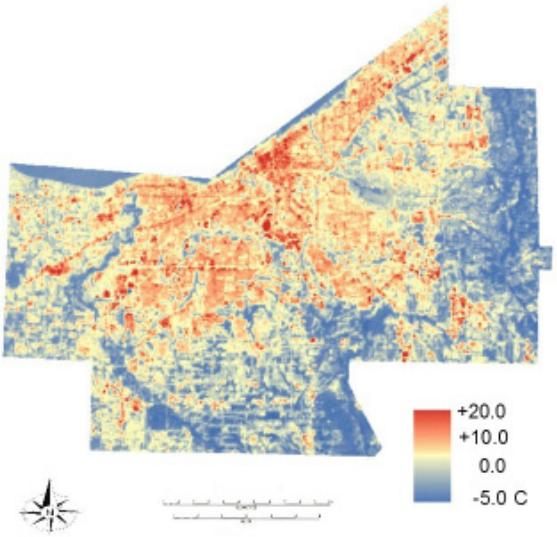

Figure 5: Spatial distribution of waste heat.

Waste Heat Class	Land Cover Class
0 = -5.0 to 3.0	1 = Industrial/ Commercial Built-up Area
1 = 3.0 to 5.0	2 = Residential/ Mixed
2 = 5.0 – 10.0	3 = Road/ Impervious Surface
3 = 10.0 – 20.0	4 = Vegetated Tree Cover
	5 = Vegetated Grass/Parkland (medium density vegetated cover)
	6 = Water
	7 = Soil/Barren (low density vegetated cover)
	0 = Unclassified

Table 4: "Waste" Heat and Land Cover Legend Categories.

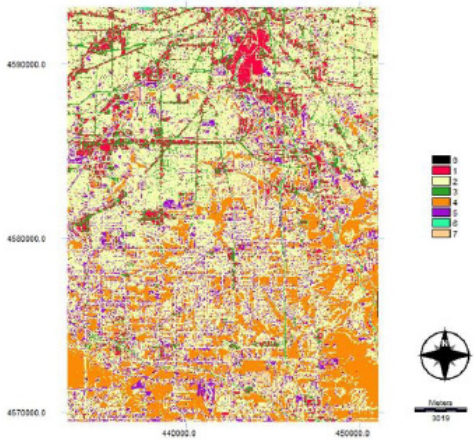

Figure 6: Analytic window displaying spatial distribution of land cover (Table 4 for legend explanation).

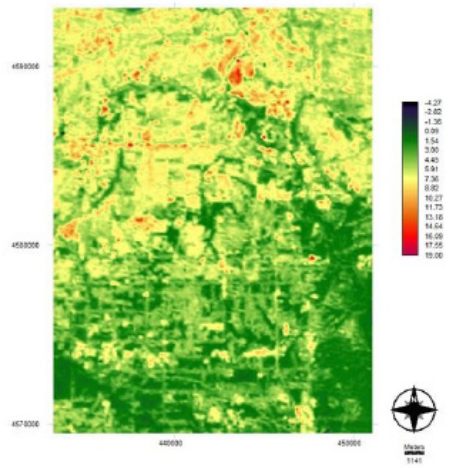

Figure 7: Spatial distribution of waste heat degrees Celsius.

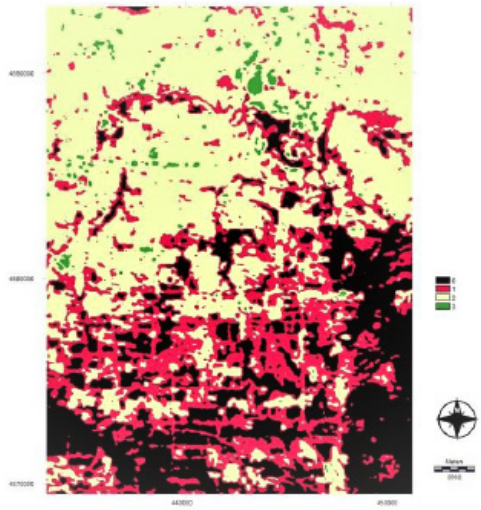

Figure 8: Reclassified waste heat surface (Table 4 for legend explanation).

To form a more detailed understanding of the association between heating excess and land cover a cross tabulation analysis was performed using the land cover and waste heat data layers. Cross-image tabulation compares the categories of land cover against the four waste heat classes. Two cross-image tabulations were conducted. The initial analysis compared the four waste heat categories across the all land cover classes (Figure 8). Industrial and related built up areas (category 1) together with residential areas (category 2) and impervious road surfaces (category 3) displayed the strongest associations with waste heat classes from 5 to 20°C above ambient air temperature (Figure 9). Road, impervious surface and industrial/commercial areas corresponded well with waste heat excesses above 10°C as did the soil and barren land cover categories (Table 5). These associations are highlighted in bold type on (Table 5). The pattern between land cover and waste heat was significant (p=0.00) with an association of 0.45 based on the Cramer's V statistic. While waste heat is an observable function of land cover, where in the spatial pattern these relationships most pronounced cannot be determined from the cross-tabulation table alone.

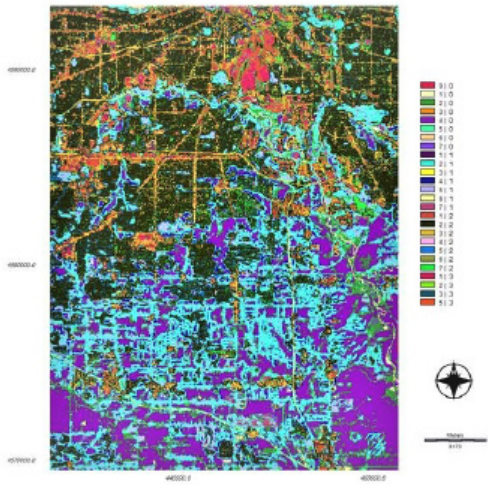

Figure 9: Full cross-image tabulation results land cover (left) waste heat (right) columns.

	0	1	2	3	4	5	6	7	Total
0	68	1209	25519	236	68380	7442	1094	1437	105385
1	0	2230	72065	2598	18001	24580	642	5367	125483
2	0	26177	145842	31101	1514	13283	464	14114	232495
3	0	4767	360	1344	0	8	20	586	7085
Total	68	34383	243786	35279	87895	45313	2220	21504	470448

Table 5: Cross Tabulation of 2015 Land Cover (columns) Against Excess Heat (rows).

Chi Square = 286018.84375
df = 21
P-Level = 0.0000
Cramer's V = 0.4502

Highlighting the spatial distribution and concentration of waste heat generation was accomplished through a series of selections that were made from the cross-image results. Focusing on waste heat conditions 10 to 20°C above ambient air temperature, the analysis highlighted the spatial distribution of industrial and impervious/barren land cover classes (Figure 10). Impervious and industrial/commercial areas displayed the highest proportion of cells in the image that corresponded to the maximum waste heat

category (highlighted in bold) with smaller contributions from the residential and soil/barren land cover classes (Table 6). Geographically, these regions show a strong spatial grouping toward the portions of the study window that define zones within the urban core of the region and trend to the west following major portions of the road system (Figure 11).

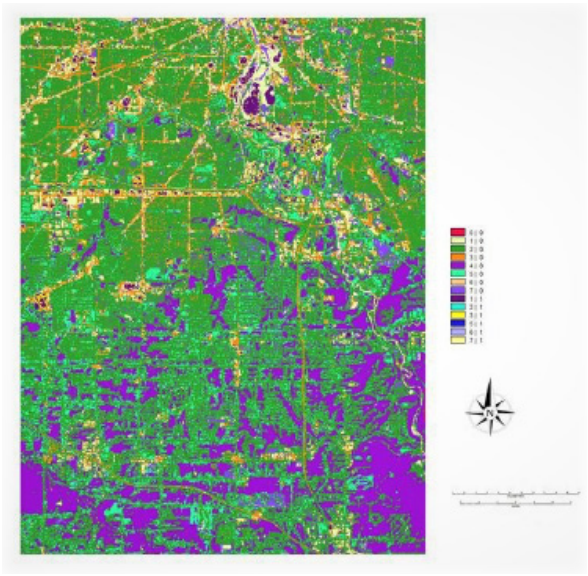

Figure 10: Cross-image tabulation results displaying selected zones of land cover (right column) against maximum waste (heat left column).

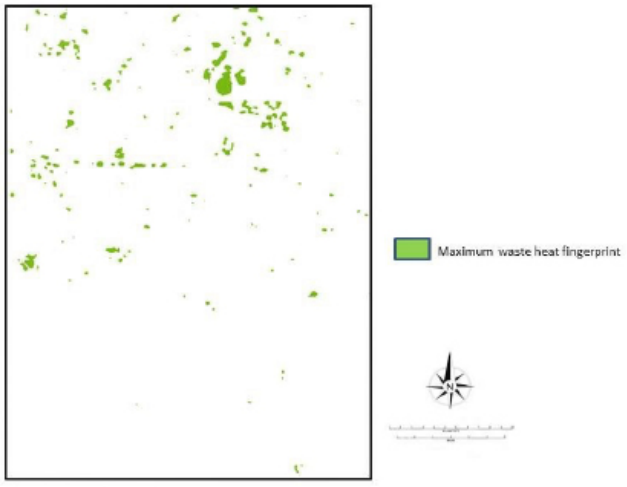

Figure 11: Selected zones highlighting spatial distribution of maximum waste heat.

	0	1	2	3	4	5	6	7	Total
0	68	29616	243426	33935	87895	45305	2200	20918	463363
1	0	4767	360	1344	0	8	20	586	7085
Total	68	34383	243786	35279	87895	45313	2220	21504	470448

Table 6: Cross Tabulation of 2015 Land Cover (columns) Against Maximum Waste Heat (rows).

Chi Square = 41939.33594
df = 7
P-Level = 0.0000
Cramer's V = 0.2986

Selecting individual combinations of land cover and fingerprint categories, as explained through the cross image analysis, facilitates visual evaluation of the spatial arrangement, location and extent f the waste heat pattern. The individual data layers produced from this exercise offers actionable data to support decision regarding the formulation of mitigation priorities and the broad issues related to jurisdictional aspects of regional land use planning. For instance, the impact of road surface and the density of impervious surface can be observed by relating these land cover categories to their defining waste heat class (Figure 12). In this example, the resulting map layer targets areas at the northern portion of the study window and reveals the heavy construction of road/impervious surface that produce excess heating patterns. Urban greening and other mitigation strategies

would be expected to focus on the areas highlighted to achieve desired reductions in anthropogenic waste heat. Similarly, mapping zones of minimum waste heat conditions identifies heavily vegetated areas in the urban landscape and demonstrates the significance of tree cover and reducing built-form density as a means to maintain or lower ambient air temperatures across the region (Figure 13). These results demonstrate a cost effective means to quantify

Figure12: Land cover contributions to waste heat formation of road/impervious surface 10-20oC above ambient temperature.

residual heat, identify the location where waste heat exceeds ambient conditions, fingerprint specific land covers that produce unsatisfactory conditions and a remote sensing methodology that supports the continuous monitoring of the urban landscape.

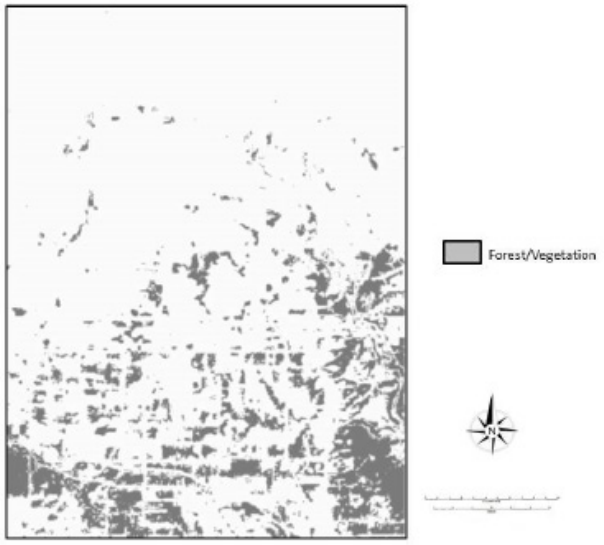

Figure 13: Land cover contributions to waste heat formation of forest/vegetation cover 5°C below ambient air temperature.

Conclusion

Elevated surface temperature is a documented phenomenon common to the urban landscape. The combination of reduced vegetated cover, low albedo surfaces and increased surface roughness are among the causal factors that produce a pattern of micro-climate distinct from surrounding non-urban areas. The urban surface, defining a composition and configuration of materials of varying densities, contrasts significantly from natural ecosystems and generates unique and conflicting environmental patterns. Recent interest in enhancing the environmental sustainability of the urban landscape has placed focus on mitigating the adverse effects of built form and related human actions on the environmental system. The application of satellite remote sensing has played a pivotal role in the analysis, and monitoring of the urban pattern and its impact on the environmental system. One important contribution has been the capacity of remotely sensed data to broaden understanding of urban thermal pollution and monitor changes within the urban landscape. Within this application area, the question of anthropogenic waste heat, its relation to land cover and the role of remotely sensing technology to produce actionable data to guide mitigation planning has not been addressed. In this paper research was conducted to demonstrate the feasibility of employing moderate resolution earth observational data to fingerprint waste heat patterns in an urban setting. Urban waste heat was defined as a thermal condition above the nominal ambient air temperature recorded at the approximate time of satellite overpass produced by kinetic temperature radiating skyward from a given surface.

Using the thermal infrared sensor of the Landsat 8 TIRS, a methodology was introduced that provided a snap-shot documentation of waste heat that was analyzed using GIS operations. GIS processing delineated zones in the urban pattern of waste heat excess and related those patterns to specific land cover types and arrangements. This approach highlighted the sources of excess and enabled the spatial "fingerprinting" of the observed waste heat anomalies to be more clearly understood. The observed association between land cover and waste heat was statistically significant and revealed the important contribution of dense urban pattern on the spatial distribution of waste heat. Individual selections made via GIS from cross-image tabulation identified specific locations in the study area where mitigation efforts could focus. The flexibility of this approach allows combinations of waste heat categories to be compared to individual land cover types to better inform the decision making process. Through the introduction of the 'waste heat" concept and the application of thermal remote sensing, this study extends research on the urban heating phenomena, providing a methodology to guide the implementation mitigation programs at a regional scale that: 1) quantifies residual/waste heat, 2) identifies specific locations of maximum waste heat, and 3) facilitates continuous monitoring of waste heat mitigation programs at a synoptic scale in a cost-effective manner.

References

1. Bornstein RD (1968) Observations of the urban heat island effect in New York City. Journal of Applied Meteorology 7: 575-582.
2. Price JC (1979) Assessment of the urban heat island effect through the use of satellite data. Monthly Weather Review 107: 1554-1557.
3. Imhoff ML, Zhang P, Wolfe RE, Bounoua L (2010) Remote sensing of the urban heat island effect across biomes in the continental USA. Remote Sensing of Environment 114: 504-513.
4. Zhao X, Jiang H, Wang H, Zhao J, Qiu Q, et al. (2013) Remotely sensed thermal pollution and its relationship with energy consumption and industry in a rapidly urbanizing Chinese city. Energy Policy 57: 398-406.
5. Dolgikh II, Pokhodun AI, Chistyakov YA (1997) Conception of metrological assurance for monitoring environmental thermal pollution. Measurement techniques 40: 1176-1179.
6. Martos A, Pacheco-Torres R, Ordóñez J, Jadraque-Gago E (2016) Towards successful environmental performance of sustainable cities: Intervening sectors. A review. Renewable and Sustainable Energy Reviews 57: 479-495.
7. Maimaitiyiming M, Ghulam A, Tiyip T, Pla F, Latorre-Carmona, et al. (2014) Effects of green space spatial pattern on land surface temperature: Implications for sustainable urban planning and climate change adaptation. ISPRS Journal of Photogrammetry and Remote Sensing 89: 59-66.
8. Nuruzzaman M (2015) Urban Heat Island: Causes, Effects and Mitigation Measures - A Review. International Journal of Environmental Monitoring and Analysis 3: 67-73.
9. Shahmohamadi P, Che-Ani AI, Ramly A, Maulud KNA, Mohd-Nor MFI (2010) Reducing urban heat island effects: A systematic review to achieve energy consumption balance. International Journal of Physical Sciences 5: 626-636.
10. Mirzaei PA, Haghighat F (2010) Approaches to study urban heat island - Abilities and limitations. Building and Environment 45: 2192-2201.
11. Voogt JA, Oke TR (2003) Thermal remote sensing of urban climates. Remote Sensing of Environment 86: 370-384.

12. Nunez M, Oke TR (1977) The energy balance of an urban canyon. Journal of Applied Meteorology 16: 11-19.
13. Nunez M, Oke TR (1980) Modeling the daytime urban surface energy balance. Geographical Analysis 12: 373-386.
14. Oke TR (1988) The urban energy balance. Progress in Physical geography 12: 471-508.
15. Zhou W, Huang G, Cadenasso ML (2011) Does spatial configuration matter? Understanding the effects of land cover pattern on land surface temperature in urban landscapes. Landscape and Urban Planning 102: 54-63.
16. Aflaki A, Mirnezhad M, Ghaffarianhoseini A, Ghaffarianhoseini A, Omrany H, et al. (2017) Urban heat island mitigation strategies: A state-of-the-art review on Kuala Lumpur, Singapore and Hong Kong. Cities 62: 131-145.
17. Coseo P, Larsen L (2014) How factors of land use/land cover, building configuration, and adjacent heat sources and sinks explain Urban Heat Islands in Chicago. Landscape and Urban Planning 125: 117-129.
18. Santamouris M, Synnefa A, Karlessi T (2011) Using advanced cool materials in the urban built environment to mitigate heat islands and improve thermal comfort conditions. Solar Energy 85: 3085-3102.
19. Santamouris M (2014) Cooling the cities - A review of reflective and green roof mitigation technologies to fight heat island and improve comfort in urban environments. Solar Energy 103: 682-703.
20. Karteris M, Theodoridou I, Mallinis G, Tsiros E, Karteris A (2016) Towards a green sustainable strategy for Mediterranean cities: Assessing the benefits of large-scale green roofs implementation in Thessaloniki, Northern Greece, using environmental modelling, GIS and very high spatial resolution remote sensing data. Renewable and Sustainable Energy Reviews 58: 510-525.
21. Tan Z, Ka-Lun Lau K, Ng E (2016) Urban tree design approaches for mitigating daytime urban heat island effects in a high-density urban environment. Energy and Buildings 114: 265-274.
22. Lanza K, Stone B (2016) Climate adaptation in cities: What trees are suitable for urban heat management? Landscape and Urban Planning 153: 74-82.
23. Li X, Zhou W, Ouyang Z (2013) Relationship between land surface temperature and spatial pattern of greenspace: What are the effects of spatial resolution? Landscape and Urban Planning 114: 1-8.
24. Susca T, Gaffin SR, Dell'Osso GR (2011) Positive effects of vegetation: Urban heat island and green roofs. Environmental Pollution 159: 2119-2126.
25. Norton BA, Coutts AM, Livesley SJ, Harris RJ, Hunter AM, et al. (2015) Planning for cooler cities: A framework to prioritise green infrastructure to mitigate high temperatures in urban landscapes. Landscape and Urban Planning 134: 127-138.
26. Lein JK (2012) Environmental Sensing: Analytical Techniques for Earth Observation. Springer-Verlag New York, USA. Pg no: 334.
27. Avdan U, Jovanovska G (2016) Algorithm for Automated Mapping of Land Surface Temperature Using LANDSAT 8 Satellite Data. Journal of Sensors 2016: 1480307.
28. Weng Q, Lu D, Schubring J (2004) Estimation of land surface temperature-vegetation abundance relationship for urban heat island studies. Remote Sensing of Environment 89: 467-483.
29. Sobrino JA, Jimenez-Munoz JC, Soria G, Romaguera M, Guanter L, et al. (2008) Land Surface Emissivity Retrieval From Different VNIR and TIR Sensors. IEEE Transactions on Geoscience and Remote Sensing 46: 316-327.
30. Hay GJ, Kyle C, Hemachandran B, Chen G, Rahman MM, et al. (2011) Geospatial technologies to improve urban energy efficiency. Remote Sens 3: 1380-1405.